The Korean Journal of Rheology,
Vol. 3, No. 2, October 1991 pp.148-155

〈연구논문〉

희석액내에서 서로 다른 길이의 분지를 가진 빗모양의 고분자 분자의 점탄성 거동에 관한 연구

서용석 · 황승상 · 김광웅

한국과학기술연구원 고분자공정연구실

(1991년 9월 7일 접수)

A Study on the Viscoelastic Behavior of Dilute Solutions of Comb-Shaped Non-equal-Length Branched Polymers

Yongsok Seo, Seung Sang Hwang and Kwang Ung Kim

Polymer Processing Laboratory, KIST, P.O. Box 131, Cheongryang, Seoul 130-650, Korea

(Received September 7, 1991)

요 약

본 연구에서는 빗모양의 고분자분자가 희석용액 상태에 있을 때의 점탄성 거동을 이론적으로 해석하였다. 수치해석 방법으로는 Osaki 등이 제안한 방법을 따랐다. 고분자분자의 이완시간은 Eigenvalue equation을 풀어서 구하였으며 고분자분자와 용매간의 역학은 Zimm-Kilb model을 적용하였다. 본 연구에서는 분지쇄의 길이가 다른 경우 이들이 분자쇄 거동에 미치는 영향을 고찰하였으며 높은 진동수에서의 현상을 해석하였다.

Abstract—In this study, viscoelastic behaviour of comb-shaped polymer molecule in dilute solution was theoretically investigated. Adopted numerical scheme follows that of Osaki *et al*'s method. Relaxation time spectrum was calculated by solving the eigenvalue equation which came from Zimm-Kilb theory for the interaction between the polymer molecule and solvent. Based on the numerical results, the effect of branch length and polymer molecule's behavior at high frequency were discussed.

Keywords: Non-equal length branched polymers, Viscoelastic behavior, High frequency, Bead-springs model.

1. Introduction

Effects of macromolecular structure on the flow behavior are very serious from a practical stand point of view. The melt-processing properties of commercial polymers can be adjusted over wide ranges by alterations in the average moleuclar weight, molecular weight distribution, and frequency of long branches in the molecule. When the molecules are branched, the polymeric fluid behavior varies with the number, location, and length of branches. Their lengths are not generally uniform like ideal branched polymers. Even though there were some studies about the mixture properties of different branch length polymers, rheological behavior of unequal length branches on the same molecule was not investigated in detail, especially at high frequencies. In this study, we investigate the various properties of polymers which have different length branches on the same back-

bone but no macrocyclic rings. This study is based on the molecular theory. Molecular theories for the viscoelastic properties of very dilute solution of branched polymers based on the bead spring model of flexible polymer molecules have been studied for many years, numerically and experimentally[1, 2]. In the present paper, we use the modified Zimm-Kilb theory adopted by Osaki *et al*[3] to treat comb-shaped polymers with certain specific geometries of nonequal length branches. The numerical calculations follow Osaki *et al*'s method.

2. Numerical Calculations

According to Zimm and Kilb theory, the reduced intrinsic complex modulus $[G^*]_R$ is defined and related to the complex shear modulus as follows:

$$[G^*]_R=[G']_R+i[G'']_R$$
$$=\lim_{c\to 0}\ (M/cRT)[G'+i(G''-\omega\eta_S)] \qquad (1)$$

where c is the concentration, M the molecular weight, R the gas constant, T the absolute temperature, ω the angular frequency, and η_s the solvent viscosity. As in the Zimm theory, $[G']_R$ and $[G'']_R$ are given as functions of the reduced frequency as follows:

$$[G']_R=\sum_{p=1}^{N}\omega_R^2(\tau_p/\tau_1)^2/[1+\omega_R^2(\tau_p/\tau_1)^2] \qquad (2)$$

$$[G'']_R=\sum_{p=1}^{N}\omega_R(\tau_p/\tau_1)/[1+\omega_R^2(\tau_p/\tau_1)^2] \qquad (3)$$

where τ_p is the pth relaxation time given by

$$\tau_p=\zeta/2\ k\lambda_p \qquad (4)$$

Here, ζ is the friction coefficient of a bead, ω_R is the reduced frequency the same as $\omega\tau_1$ and k is the spring constant ($k=3kT/b^2$ where b^2 is the mean square length of the spring). The quantity λ_p is the pth eigen value of the H·A matrix defined for the comb geometry; the H matrix describes the hydrodynamic interaction between beads and the A matrix represents the spring forces on the beads (See appendix for details). The matrix involves the hydrodynamic interaction parameter h* defined as follows:

$$h^*=\zeta/(12\pi^3)^{0.5}\ b\ \eta_s \qquad (5)$$

Dimensions of H and A matrices are varied depending on each branch bead numbers. The eigenvalues were calculated using IMSL subroutine EVLSF. Similarity transformation was also used for efficient algorithm[4].

3. Results and Discussion

In evaluating eigenvalues, there are two adjustable parameters, h* and total beads number N. For comb-shaped polymers, since molecular symmetry does not exist, the total number of beads N should be large. Using super computer Cray-2 we can take very large values of N. To save computational time, N was limited less than 1000 which is considered enough for our analysis. To check the accuracy of our code some exemplary tests were done to compare with Osaki *et al*'s results. Present program produces exactly the same as those cited in reference 3.

Nonequal length branched polymers are investigated by varying the number of beads on each branch. The number of beads between the branches was set as 30. Total number of branches was fixed at 10. The long branch bead number was set as 30 and short branch bead number was set at 5. In this study we put a limit on the length of long branches, not longer than branch point distance on the backbone because, if the branch length is too long, the molecule structure might be approximated better by star-comb shape polymers rather than comb-shape polymers.

Fig. 1 and 2 show the behavior of reduced storage and loss modulus when the hydrodynamic interaction is negligible (Rouse dynamics) and when it is dominant (Zimm dynamics). As well known, the reduced intrinsic moduli as functions of ω_R are independent of M as long as it is not too large, since the sums are essentially independent of N, the arbitrary number of submolecules, i. e., they are indistinguishable from the corresponding sums with $N=\infty$. As presented in equa-

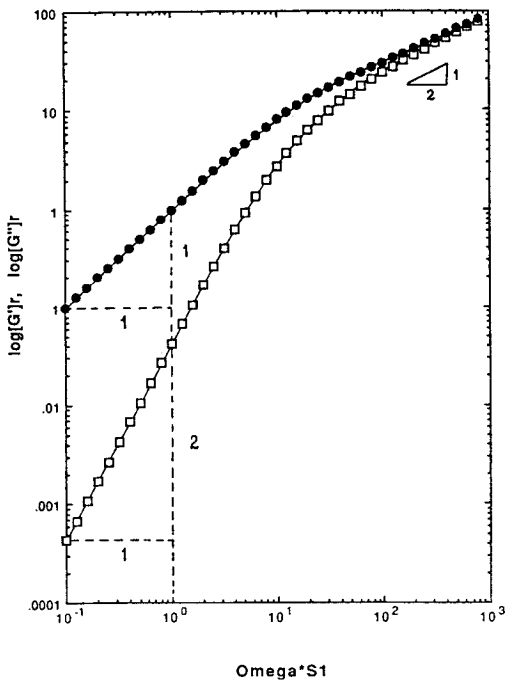

Fig. 1. Logarithmic plots of $[G']_R$ and $[G'']_R$ vs ωS_1 for a linear molecule when hydrodynamic interaction is negligible. h*=0 (following Rouse theory)
□Storage modulus; ●Loss modulus.

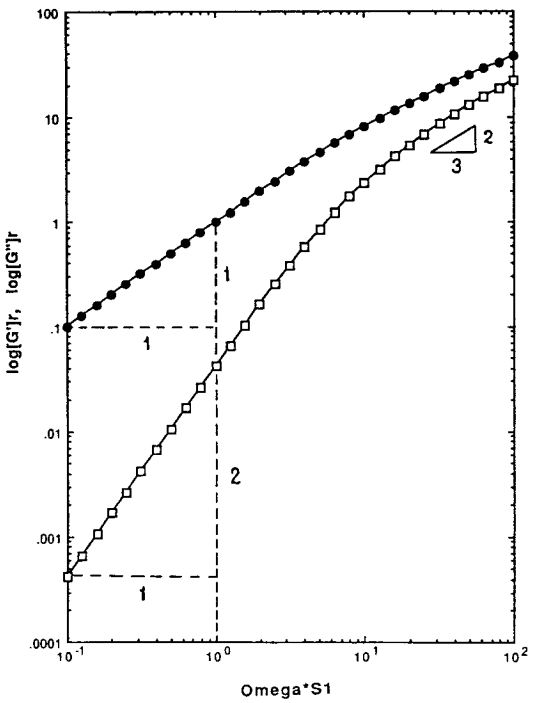

Fig. 2. Logarithmic plots of $[G']_R$ and $[G'']_R$ vs ωS_1 for a linear molecule when hydrodynamic interaction is dominant. h*=0.25 (following Zimm theory)
□Storage modulus; ●Loss modulus.

tions (2) and (3), when hydrodynamic interaction is negligible (Rouse dynamics) reduced storage modulus is proportional to the second power of ω_R while reduced loss modulus is proportional to the first power of ω_R in low frequency region. In high frequency range, both reduced moduli show the slope of 1/2 as expected. On the other hand, when the hydrodynamic interaction is dominant, the slopes in low frequency range is 1 and 2 for reduced loss modulus and storage modulus respectively, but the slope on the logarithmic plot at higher frequencies is 2/3 and reduced storage modulus and loss modulus are not equal but differ by a factor of $\sqrt{3}$ (Ferry[5]). These facts are well represented in Fig. 1 and 2. In Fig. 2, the slopes at high frequency are not exactly parallel because hydrodynamic interaction parameter is not enough big (h*=0.25). In dominant hydrodynamic interaction regime, the slope of modulus on the logarithmic plot at higher frequency is 2/3 since all τ_p except the first few are proportional to $p^{-2/3}$ whereas they are proportional to p^{-2} in free-draining case (negligible hydrodynamic interaction).

Generally it is well known that branched polymers have a lower viscosity than that of linear polymers of the same molecular weight. At low concentration, the viscosity ratio of branched polymer to linear polymer depends primarily on the ratio of gyration, $g'=S_B^2/S_L^2$. This parameter was calculated from eq. (32) of Zimm-Kilb paper[3]. According to it,

$$g'=\left(\sum_{k=1}^{\infty} 1/\lambda_k\right)_{branched}\left(\sum_{k=1}^{\infty} 1/\lambda_k\right)^{-1}_{linear} \quad (6)$$

Inverse of the smallest eigenvalue, $1/\lambda_1$, corresponding to longest relaxation time is presented in Fig. 3. It decreases with the fraction of short chain when the value of h* was set as 0.25. Calculated g′ is shown in Fig. 4. As we know, g′ increases

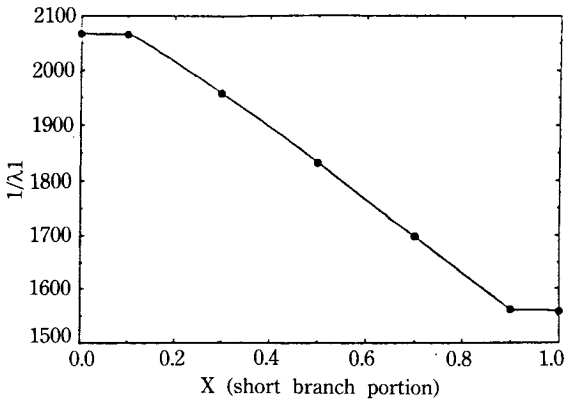

Fig. 3. Inverse of the smallest eigenvalue corresponding to the longest relaxation time vs short branch portion when h*=0.25.

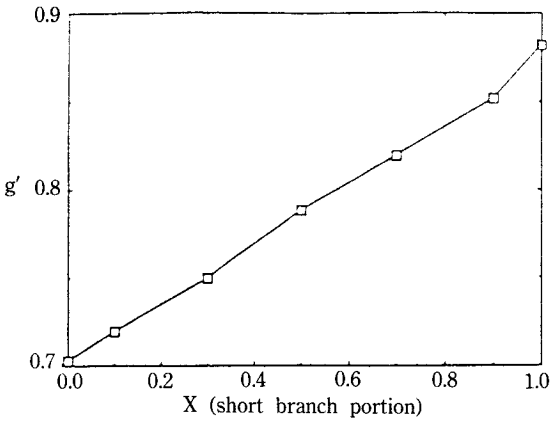

Fig. 4. Ratio of the square of radius of gyration vs short branch portion.

with short chain fraction which means the molecular structure resembles that of the linear molecule. Even though they are not exactly on the straight line, we can see that g′ rises almost linearly with short chain fraction except near the portion of 0.1 where the molecule structure is almost the same as a linear polymer.

Plots of $[G']_R$ and $[G'']_R$ vs log ωS_1 are shown in Fig. 5 and 6 where S_1 is defined as

$$S_1 = \sum_{p=1}^{N} \tau_p/\tau_1 \qquad (7)$$

$[G']_R$ reaches almost a constant value at high frequency range whereas $[G'']_R$ reaches a maximum at some frequency and then decreases. At high

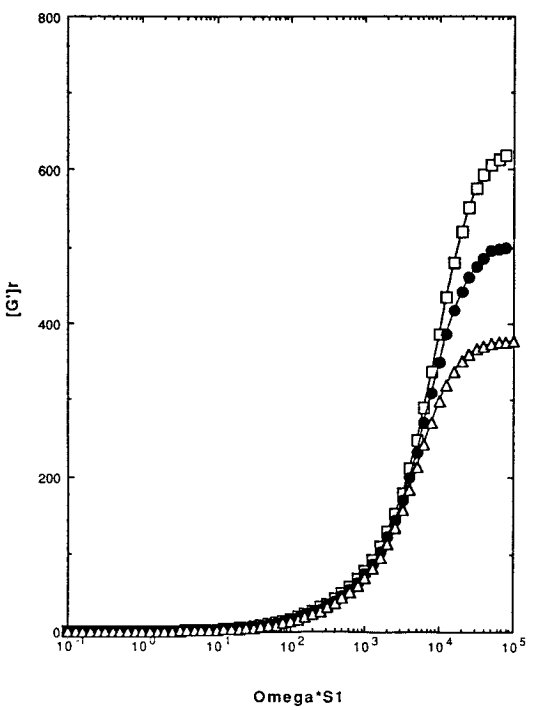

Fig. 5. Reduced storage modulus vs ωS_1 when h*= 0.25.
□ All long branches; ● Half long branches; △ All short branches.

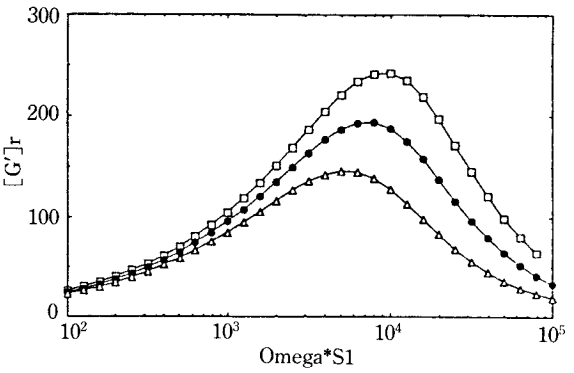

Fig. 6. Reduced loss modulus vs ωS_1 when h*= 0.25.
□ All long branches; ● Half long branches; △ All short branches.

frequency, individual molecules are stretched, according to the beads-and-springs model. A crossover from $G''\sim\omega^{2/3}$ to $G''=\eta_s\omega$ is therefore predicted. In the beads-and-springs description, a polymer molecule contributes nothing to the viscous

dissipation if the deformation is too fast even the submolecules to relax. Then, the polymer contribution to the dynamic viscosity, which is defined as $\eta_p' = G''/\omega - \eta_s$ is ideally predicted to approach zero at high frequency as shown in Fig. 12 later [6]. As ω increases, all elastic motions available to the molecule are eventually exhausted, and G' reaches a plateau. Even though η_p' should have zero value at high frequency, in real dilute polymer solutions, short segments of polymer act like rigid structures past which solvent must flow, thereby exerting drag and dissipating energy because it is unable to deform. In this high frequency limit, the dilute solution then acts like a suspension of rigid particles, and $\eta' = G''/\omega$ approaches a constant value. As mentioned by Larson[6], the true situation is no doubt more complicated than this, with a role being played by specific steric and energetic interactions between polymer and solvent. Depending on its interactions with the solvent, a polymer can either reduce or enhance solvent structure, thereby affecting its ability to dissipate energy. The maximum peak position in Fig 6 moves to low frequency side with increasing short branch portion, which means the relaxation times of the chain decreases with more short branches.

The change of h* value affects the behaviours of $[G']_R$ and $[G'']_R$. Increase of interaction parameter reduces polymer relaxation times. This implicates the effect of hydrodynamic interaction is to shorten the longer relaxation times and thereby compress the relaxation spectrum. So, $[G']_R$ reaches a plateau value at lower frequency and $[G'']_R$ reaches the peak value at lower frequency as shown in Fig 7 and 8. Fig 9 compares the storage moduli at high frequency with different interaction parameters.

An important parameter governing elastic response is J_e^0, the steady-state recoverable shear compliance. Broadly speaking, J_e^0 characterizes the elastic recoil that occurs when the external forces producing a steady flow are suddenly removed. In steady shear flow the shear stress, σ, and the amount of shear recovery γ_r, are related by $\gamma_r = J_e^0\sigma$. One expects to find smaller values of J_e^0 for branched polymers. In dilute solutions J_e^0 for branched polymers is indeed smaller than that of linear polymers and it is also true with the polymer

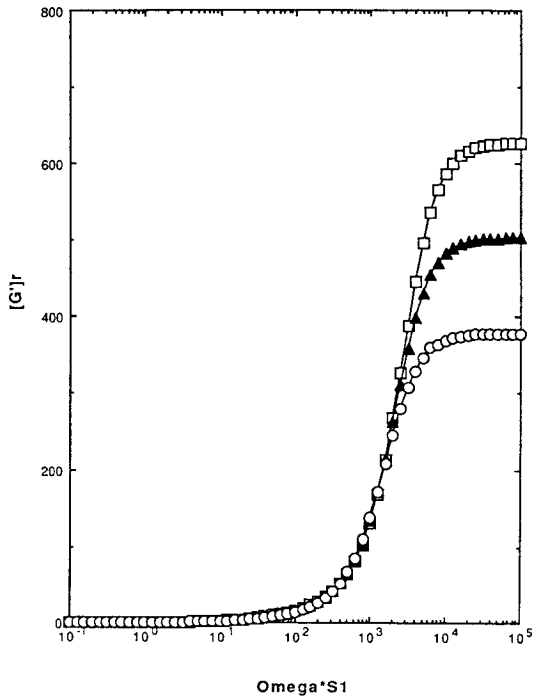

Fig. 7. Reduced storage modulus vs ωS_1 when h*= 0.49.
□ All long branches; ● Half long branches; △ All short branches.

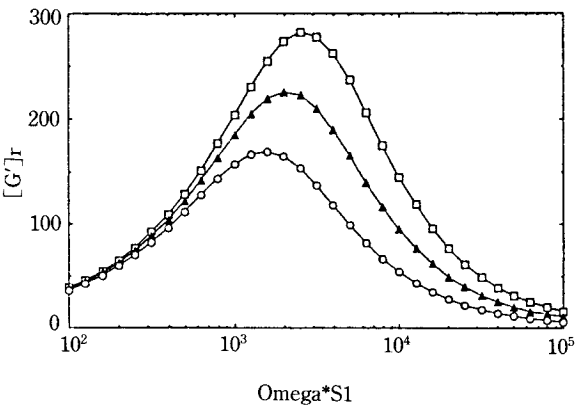

Fig. 8. Reduced loss modulus vs ωS_1 when h*= 0.49.
□ All long branches; ● Half long branches; △ All short branches.

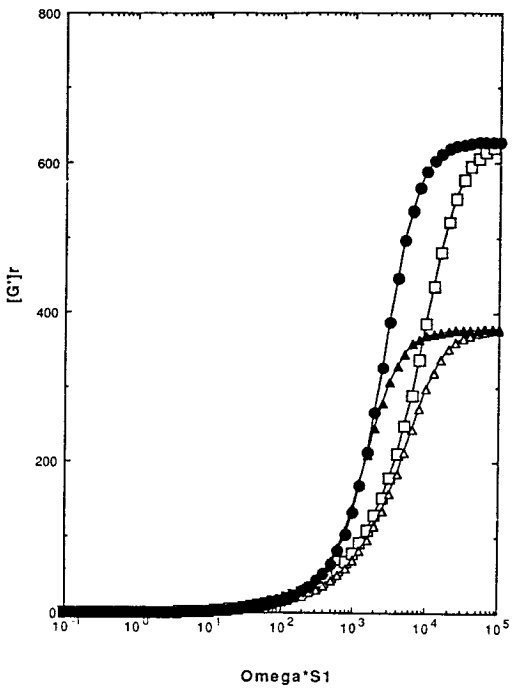

Fig. 9. Reduced storage modulus vs ωS_1. □ All long branches when h*=0.25; △ All short branches when h*=0.25; ● All long branches when h*=0.49; ▲ All short branches when h*=0.49.

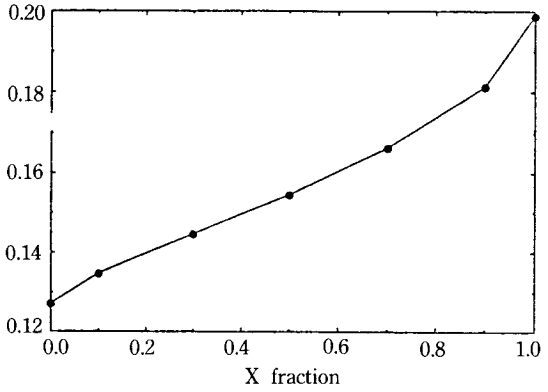

Fig. 10. Reduced steady state recoverable shear compliance vs short branch portion.

having short branches. The reduced steady-state recoverable shear compliance can be obtained from the ratio of S_2/S_1^2 where S_2 is defined as

$$S_2=\sum_{p=1}^{N}(\tau_p/\tau_1)^2 \tag{8}$$

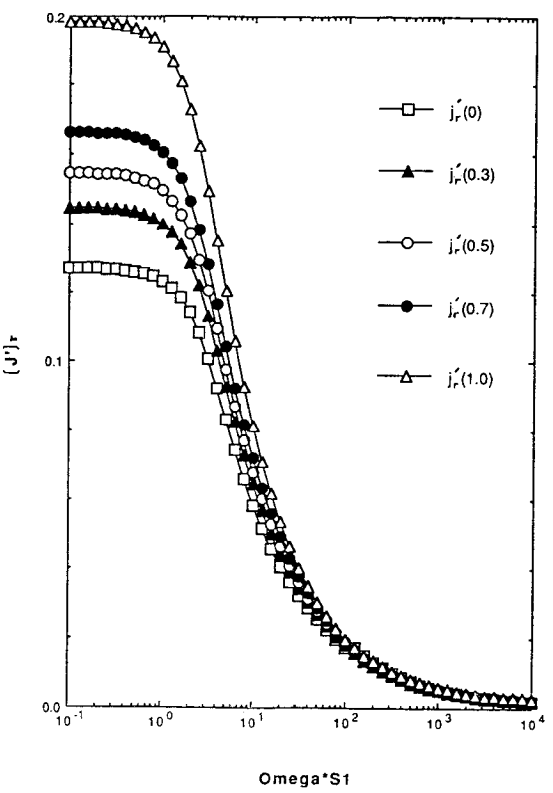

Fig. 11. Reduced storage compliance vs ωS_1 (the number in the parenthesis means the short branch portion).

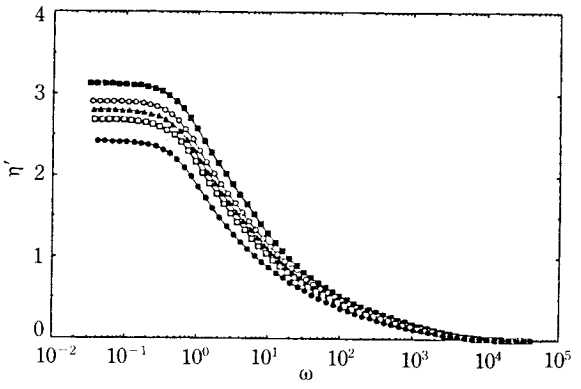

Fig. 12. Real part of reduced complex viscosity vs ωS_1. Short branch portion is ■=0, ○=0.3, ▲=0.5, □=0.7, ●=1.0.

It is shown in Fig 10 against short chain fraction. Since storage modulus decreases with short chain fraction, J_e^0 increases with it. J_e^0 can be obtained in another way as

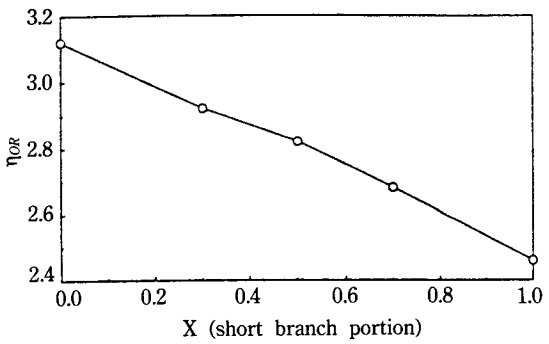

Fig. 13. Reduced steady state viscosity at zero shear rate.

$$J_e^0 = \frac{1}{\eta_0^2}\int_0^\infty t\ G(t)\ dt = \lim_{\omega\to 0}\ \frac{G'(\omega)}{|G^*(\omega)|^2} \tag{9}$$

where η_0 is the steady-state viscosity at zero shear rate. The reduced storage compliance $J'(\omega)=G'(\omega)/|G^*(\omega)|^2$ is plotted as a function of ωS_1 in Fig 11. The behavior of J_e^0 is very sensitive to short branch fraction. Also from Fig 11, we can see that it rises steeply when the polymer molecule structure resembles that of a linear polymer, i.e, when the short branch fraction reaches 1. This is similar to the behavior of the square of radius of gyration. In the mean fraction they rise almost linearly. Fig 12 shows the real part of reduced complex viscosity vs ωS_1. As we can see it reaches a constant value at high frequency. This agrees with previous interpretation of the behavior of G′ and G″ at high frequency. The values of reduced steady-state viscosity at zero shear rate can be obtained from this figure because

$$\eta_{0R} = \int_0^\infty G(t)\ dt = \lim_{\omega\to 0}\ \frac{G''(\omega)}{\omega} \tag{10}$$

In decreases almost linearly with the short branch fraction as shown in Fig 13.

4. Concluding Remarks

We briefly look at the behavior of dilute comb-shape polymers which have different length branches on their backbone. Generally, the behaviour of unequal length branched comb-shape polymers resembles that of binary blends of different molecular weight polymers in many points[7]. When they have different length branches, their viscoelastic properties changes almost linearly with short branch fraction except near 1 where the polymer structure resembles that of linear polymers, which brings about the rapid property change. The results imply that overall structure of branched polymers cannot be exactly determined from rheological property measurement alone and experimental result only represents their averaged superficial behavior. Comb-shaped branched polymer's behavior at high frequency reminds the importance of interaction parameter depending on which a polymer can either reduce or enhance solvent structure, thereby affecting its ability to dissipate energy, since strong hydrodynamic interaction effect is to shorten the longer relaxation times and thereby compress the relaxation spectrum.

References

1. J. Roovers and P.M. Toporowski, *Macromolecules* **20**, 2300 (1987); J. Roovers and W.W. Graessley, *Macromolecules* **14**, 766 (1981).
2. R.T. Bailey, A.M. North and R.A. Pethrick "Molecular Motion in High Polymers" Clarendon Press, Oxford, (1981).
3. K. Osaki, Y. Mitsuda, J.L. Shrag and J.D. Ferry, *Trans. Soc. Rheol.* **18**, 395 (1974); B.H. Zimm and R.W. Kilb, *J. Polym. Sci.*, **37**, 19 (1969).
4. A.S. Lodge and Y.J. Wu., *Rheol. Acta*, **10**, 539 (1971).
5. J.D. Ferry "Viscoelastic Properties of Polymers" 3rd edn, John Wiley & Sons Inc. New York, (1980).
6. R.G. Larson "Constitutive Equations for Polymer Melts and Solutions" Butterworths, Boston, 1988.
7. M.J. Struglinski and W.W. Graessley, Macromolecules, **18**, 2630 (1985); H. Watanable and T. Kotaka, *Macromolecules*, **17**, 2316-2325 (1984).

Appendix

In Zimm-Kilb model calculation of relaxation times is from characteristic equation of $H\cdot A=\lambda I$ where H matrix describes the hydrodynamic interaction between beads. The H matrix includes the

hydrodynamic interaction parameter h* defined below (See reference 3 for the derivation of these equations). When we set N_f as the number of branches, N_{bi} the number of beads on branch i, N_s-1 the number of beads between branch points, N_0 the number of beads on the backbone ($N_o=(N_f+1)N_s-1$), the total number of the beads $N=N_o+$sum of N_{bi}, the size of H and A are N×N. The H matrix for a comb polymer is

$$H=\begin{bmatrix} H_{-1} & H_{m1} & H_{m2} & \cdot & \cdot & H_{mf} \\ H_{m1}^T & H_{-2} & H_{b12} & \cdot & \cdot & H_{b1f} \\ H_{m2}^T & H_{b12}^T & H_{-2} & \cdot & \cdot & H_{b2f} \\ \cdot & \cdot & \cdot & \cdot & \cdot & \cdot \\ \cdot & \cdot & \cdot & \cdot & \cdot & \cdot \\ \cdot & \cdot & \cdot & \cdot & H_{-2} & H_{bf-1,f} \\ H_{mf}^T & H_{b1f}^T & H_{b2f}^T & \cdot & H_{bf-1,f}^T & H_{-2} \end{bmatrix}$$

where

$H_{-1}(i, j)=\delta_{ij}+(1-\delta_{ij})h^*(2/|i-j|)^{1/2}$
i, j=1 to N_o
$H_{-2}(i, j)=\delta_{ij}+(1-\delta_{ij})h^*(2/|i-j|)^{1/2}$
i, j=1 to N_{bf}
$H_{mk}(i, j)=h^*(2/[j+|i-k\ N_s|])^{1/2}$
i=1 to N_o, j=1 to N_{bf}
$H_{bkl}(i, j)=h^*(2/[i+j+|k-l|N_s])^{1/2}$
i=1 to N_{bf}, j=1 to N_{bf} k, l=1 to N_f

and $h^*=\zeta/(12\pi^3)^{1/2}$ b η_s hydrodynamic interaction coefficient. The A matrix represents the spring forces on the beads. The A matrix for a comb polymer is

$$A=\begin{bmatrix} A_m & a_1 & a_2 & \cdot & \cdot & a_1 \\ a_1^T & A_1 & 0 & \cdot & \cdot & 0 \\ a_2^T & 0 & A_1 & \cdot & \cdot & 0 \\ \cdot & \cdot & \cdot & \cdot & \cdot & \cdot \\ \cdot & \cdot & \cdot & \cdot & \cdot & \cdot \\ \cdot & \cdot & \cdot & \cdot & A_1 & 0 \\ a_f^T & 0 & 0 & \cdot & 0 & A_1 \end{bmatrix}$$

where A_m's components are
$A_{ii}=1$, when i=1 or N_0
3, when i=j N_s and j=1 to N_f
2, otherwise
$A_{i,\,i+1}=-1$, when i=1 to N_0-1
$A_{i+1,\,i}=-1$, when i=1 to N_0-1
$A_{i,\,j}=0$, when $j\geq i+2$ or $j\leq i-2$ with i, j=1 to N_0
and A_1's components are
$A_{ii}=2$
$A_{i,\,i+1}=-1$, when i=1 to N_0-1
$A_{i+1,\,i}=-1$, when i=1 to N_0-1
othwrwise $A_{i,\,j}=0$ and a_k's components are $a_{ij}=-1$ when i=k N_s and j=1
0 otherwise
i=1 to N_0, j=1 to N_{bk} and k=1 to N_f.
Superscript T means the transpose of the matrix.